

Lamb shift enhancement and detection in strongly driven superconducting circuits

Vera Gramich,^{1,2,*} Simone Gasparinetti,² Paolo Solinas,^{2,3} and Joachim Ankerhold¹

¹*Institut für Theoretische Physik, Universität Ulm, Albert-Einstein-Allee 11, 89069 Ulm, Germany*

²*Low Temperature Laboratory (OVLL) - Aalto University School of Science, P.O. Box 13500, 00076 Aalto, Finland*

³*SPIN-CNR - Via Dodecaneso 33, 16146 Genova, Italy*

(Dated: December 3, 2024)

It is shown that strong driving of a quantum system substantially enhances the Lamb shift induced by broadband reservoirs which are typical for solid-state devices. By varying drive parameters the impact of environmental vacuum fluctuations with continuous spectral distribution onto system observables can be tuned in a distinctive way. This provides experimentally feasible measurement schemes for the Lamb shift in superconducting circuits based on Cooper pair boxes, where it can be detected either in shifted dressed transition frequencies or in pumped charge currents.

PACS numbers: 03.65.Yz, 85.25.Dq, 32.70.Jz, 03.67.Lx

Introduction.- Quantum fluctuations of the electromagnetic vacuum affect atomic spectra [1], a phenomenon termed Lamb shift (LS) which has triggered the development of modern quantum electrodynamics (QED). Experimentally, cavity QED [2–4] has opened the door for an unprecedented level of accuracy in the manipulation and measurement of atomic quantum states [5]. Its most recent realization is circuit QED [6–8] based on a solid-state architecture consisting of a superconducting Cooper pair box (CPB) embedded in a superconducting waveguide resonator. Circuit QED has been able to reproduce several quantum optics experiments [9–11], with advantages in terms of design, fabrication and scalability giving also access to parameter ranges currently unreachable in optical setups [9–11].

Cavity and circuit QED are based on strongly modified density of states of the electromagnetic environment seen by the atom compared to a continuum. Recently, this has allowed to detect the LS also in a circuit QED set-up in form of zero-point fluctuations of a single harmonic mode of a resonator [12]. Even the creation of real photons out of the vacuum, known as the dynamical Casimir effect, has been seen [13, 14]. However, LS modifications should naturally arise in electric circuits as the devices of interest can never be isolated from their surroundings, particularly from those with broadband spectral densities. While this class of environments constitutes the most common one for solid-state systems, evidence for corresponding LS effects has proven elusive yet. Engineered environments such as those realized in atomic set-ups [15, 16] and studied for solid-state systems [17–19] may provide a solution, actual realizations pose serious challenges though.

In this Letter, we propose a different scheme for the LS detection in a solid-state system weakly interacting with a broadband environment. Instead of *engineering* the environment, the system is subject to a *strong and tunable driving field*. This drive can not be treated as a perturbation and the interaction between driven system and its environment is best described in terms of “dressed states”

that recently have attracted much attention in superconducting circuits [20–22]. Under certain resonant conditions, the system-environment coupling is substantially enhanced by the presence of the drive, yielding a dynamic steady state which is largely determined by environmental features itself [23–25]. Within the same regime, we find that the environment also induces a renormalization of the dressed-state energies (quasienergies). This renormalization defines the LS of the driven system. Its relative magnitude can be much larger than that typically observed in undriven systems and it exhibits specific scaling trends as a function of the drive parameters. These two features should make it easier to unambiguously identify the LS contribution.

While enhanced LSs should be observable in other driven solid-state systems as well [25–27], here we focus on superconducting devices and consider circuits containing CPBs. This provides direct contact to recent experiments on driven CPBs used to realize a Mach-Zehnder interferometer [20] and to operate as a charge pump [28–31]. Particularly, the latter situation reveals that the LS may also induce clear signatures in coherent charge currents.

LS of a driven two level system.- We start with a generic model, where a CPB subject to a transversal monochromatic drive can be described by a driven two level system (TLS), i.e.,

$$H_S(t) = -\frac{E}{2}\sigma_z + A [\cos(\Omega t)\sigma_x - \sin(\Omega t)\sigma_y]. \quad (1)$$

Here, E is the level spacing of the undriven system, A the drive amplitude and Ω the drive frequency. This realization is also known as the semiclassical Rabi model, first used to describe optical transitions of atoms [32]. The TLS is embedded in a reservoir and interacts via $H_I = S \sum_j c_j (b_j^\dagger + b_j)$ with an ensemble of bosonic modes with creation/annihilation operators b_j, b_j^\dagger . In the limit of a quasi-continuum, the reservoir is characterized by a spectral distribution of these modes $J(\omega) = (\pi/\hbar) \sum_j c_j^2 \delta(\omega - \omega_j)$. For typical solid-state systems,

this distribution has a broadband profile which here is assumed to be Ohmic-like, i.e., $J(\omega) = \eta \hbar \omega \exp(-\omega/\omega_c)$ with coupling constant η and a large cut-off frequency ω_c . Generalizations are straightforward. The system operator

$$S(r) = \sin(r) \sigma_x + \cos(r) \sigma_z \quad (2)$$

is chosen such as to capture both decoherence ($r = \pi/2$) or pure dephasing ($r = 0$).

A powerful approach to treat periodically driven quantum dynamics is given by the Floquet formalism [33]. One starts from a complete set of solutions of the time-dependent Schrödinger equation for $H_S(t) = H_S(t + 2\pi/\Omega)$ given by the Floquet states $|\Psi_\alpha(t)\rangle = e^{-i\epsilon_\alpha t/\hbar} |\Phi_\alpha(t)\rangle$, where the Floquet modes $|\Phi_\alpha\rangle$ satisfy $|\Phi_\alpha(t)\rangle = |\Phi_\alpha(t + 2\pi/\Omega)\rangle$. The quasienergies ϵ_α play the role of dressed state energies and are only defined mod $\hbar\Omega$. The Floquet description manifestly takes into account the fundamental and all higher harmonics and thus applies also to arbitrary strong driving far from resonance. For the TLS in (1) one easily finds $\epsilon_{1,2} = (\Delta \pm \hbar\omega_R)/2$ with detuning $\Delta = E - \hbar\Omega$ and Rabi frequency $\omega_R = \sqrt{\Delta^2 + 4|A|^2}/\hbar$.

In case of weak dissipation, the Floquet formalism can be consistently combined with second order perturbation theory to arrive at a Born-Markov-type master equation for the reduced dynamics of the system $\rho(t)$ [33]. After performing a partial secular approximation [23], this master equation becomes time-independent in the basis of the Floquet modes and takes in the Schrödinger picture the form

$$\dot{\rho}_{\alpha\beta}(t) = -i(\omega_{\alpha\beta} - \delta\omega_{\alpha\beta}) \rho_{\alpha\beta}(t) + \sum_{\gamma,\delta} \mathcal{R}_{\alpha\beta\gamma\delta} \rho_{\gamma\delta}(t) \quad (3)$$

with transition frequencies $\omega_{\alpha\beta} = (\epsilon_\alpha - \epsilon_\beta)/\hbar$. The Redfield tensor $\mathcal{R}_{\alpha\beta\gamma\delta}$ captures decoherence/dephasing and formally couples equations for the populations (diagonal elements of the density) and the coherences (off-diagonal ones) (see Supplemental Material [34]). The additional term $\delta\omega_{\alpha\beta}$, neglected in previous studies [23, 33, 35], accounts at sufficiently low temperatures for environmental vacuum fluctuations and is the main focus of this work. It constitutes the LS for the driven quantum system.

Specifically, in case of a TLS at zero temperature we find $\delta\omega_{12} = (\eta\omega_c/\pi) \Lambda^{(r)}$, where

$$\Lambda^{(r)} = \sum_k g(\Delta_{21,k}/\omega_c) |X_{21,k}^{(r)}|^2 \quad (4)$$

contains dressed transition frequencies $\Delta_{\alpha\beta,k} = (\epsilon_\alpha - \epsilon_\beta)/\hbar + k\Omega$ and coupling matrix elements

$$X_{\alpha\beta,k}^{(r)} = \frac{\Omega}{2\pi} \int_0^{2\pi/\Omega} dt e^{-ik\Omega t} \langle \Phi_\alpha(t) | S(r) | \Phi_\beta(t) \rangle.$$

Reservoir properties are encoded in the anti-symmetric function $g(x) = x[\text{Ei}(x)e^{-x} + \text{Ei}(-x)e^x]$ with

$g(|x| \gg 1) \approx 2/x$, $g(|x| \ll 1) \approx 2x \ln(|x|)$. This way, the logarithmic behavior known from the atomic LS [1] is recovered in (4), e.g., in the $k = 0$ sector close to a degeneracy of the quasienergies. Finite temperature corrections are negligible in the domain, where typical experiments are operated.

The master equation (3) substantially differs from that for undriven systems in that close to a degeneracy in the Floquet spectrum (i.e., small values of $\omega_{\alpha\beta}$), the environmental induced terms can dominate the dynamics. As a matter of fact, for an Ohmic environment, the effective system-bath coupling is given by $\eta\Omega/|\epsilon_1 - \epsilon_2|$ [23] which, in contrast to the undriven case, can be large close to a crossing of the quasienergy levels. We note in passing that this does not violate the validity of (3) as the partial secular approximation near the first resonance (first Brillouin zone) only requires $\Omega \gg \eta\omega_R$ [23].

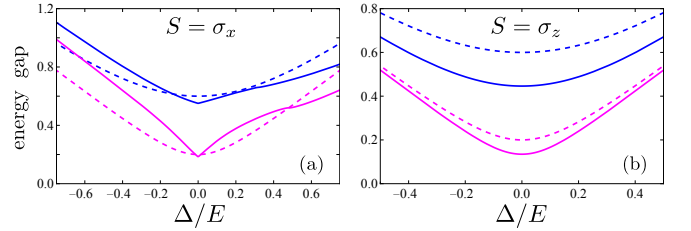


FIG. 1. Quasienergy gap $\hbar\omega_{12}/E$ of (1) with (solid) and without (dashed) LS according to (4) as a function of detuning Δ for driving amplitudes $|A|/E = 0.1$ (magenta) and 0.3 (blue), and different coupling mechanisms to the bath: (a) $S = \sigma_x$ and (b) $S = \sigma_z$. Damping parameters are $\eta = 0.1$ and cut-off frequency $\hbar\omega_c/E = 60$.

Strongly driven CPB.- Despite its simplicity, the model (1) provides not only conceptually profound insight into the impact of zero-point fluctuations but experimentally opens relatively easy access to LS measurements. This is particularly true in the regime, where the dynamics is governed by the interaction with the environment. Apparently, the LS (4) also carries information about the system (CPB)-reservoir coupling mechanism via the operator $S(r)$ in (2). In the two limiting cases referring to mixing angles $r = \pi/2$ (transversal coupling) and $r = 0$ (longitudinal coupling) one has with $\tan(2\theta) = 2|A|/\Delta$, from (4)

$$\begin{aligned} \Lambda^{(0)} &= -g(\omega_R/\omega_c) \sin^2(2\theta) \\ \Lambda^{(\pi/2)} &= g(\omega_-/\omega_c) \sin^4(\theta) + g(\omega_+/\omega_c) \cos^4(\theta) \end{aligned} \quad (5)$$

with $\omega_{\pm} = \pm\Omega - \omega_R$. Upon tuning the drive amplitude and/or frequency, the LS thus displays a qualitatively different behavior in contrast to the bare quasienergy gap. Namely, for transversal coupling ($S = \sigma_x$), the quasienergy gap of the TLS including the LS shows a pronounced asymmetry with respect to negative and positive detuning (Fig. 1a). A measurement of this deviation

from the linear scaling would be a clear signature of the presence of environmental ground state fluctuations. On the contrary, for longitudinal coupling (pure dephasing, $r = 0$) leads to a smoother structure and less deviations from the bare transition frequencies, see Fig. 1b.

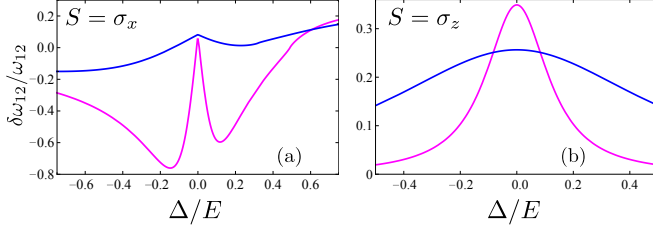


FIG. 2. Relative magnitude of the LS $\delta\omega_{12}/\omega_{12}$ for (a) transversal (σ_x) and (b) longitudinal (σ_z) coupling vs. detuning Δ and for different values of the driving amplitude $|A|/E$: 0.07 (magenta), 0.3 (blue). Other parameters are as in Fig. 1.

To have a more quantitative estimate of the impact of the LS, in Fig. 2, we plot the relative magnitude of the LS compared to the bare transition frequency when the detuning is varied. In fact, the external driving increases the ratio $|\delta\omega_{12}/\omega_{12}|$ for both coupling schemes far above the usual ratio of a few percent for autonomous systems [12]. This enhanced influence of the environment onto the system dynamics is directly related to the driving which allows the dressed system to exchange energy quanta with the bath also in multiples of $\hbar\Omega$. Environmental vacuum fluctuations are thus probed at various frequency scales in contrast to the undriven situation.

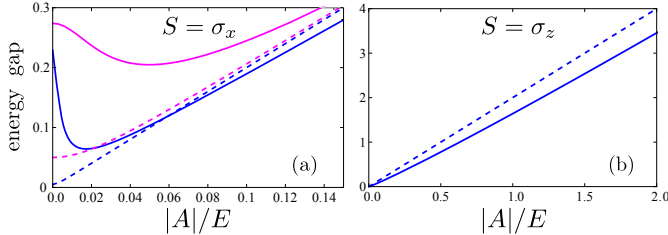


FIG. 3. Same as in Fig. 1, but vs. driving amplitude $|A|$ close to the resonance with $|\Delta|/E$: 0.005 (blue) and 0.05 (magenta). The corresponding curves in (b) cannot be resolved on this scale.

An alternative way to measure the effect of the enhanced LS by varying the drive amplitude A is presented in Fig. 3: For longitudinal coupling (b) one finds a smooth behavior, where close to resonance the dependence on $|\Delta|$ disappears and the LS vanishes for $A \rightarrow 0$. The situation for transversal coupling (a) is quite different. In this case, according to $\Lambda^{(\pi/2)}$ in (5) one has close to resonance $\delta\omega_{12}(0 < |\Delta|/E \ll 1, A = 0) \approx (2\Omega\eta/\pi)\ln(\Omega/\omega_c)$, while the bare energy gap reduces to $|\Delta|$. This leads to a highly non-monotonic dependence of the full gap on the driving amplitude and allows for a

clear discrimination between the prevalence of either of the coupling mechanisms. Note the discontinuity of the LS in the limits $|\Delta| = 0, 0 < |A|/E \ll 1$ (seen in Fig. 2a) and $0 < |\Delta|/E \ll 1, A = 0$ (seen in Fig. 3a) which is due to the θ -dependence of $\Lambda^{(\pi/2)}$.

LS detection.— We now discuss in more detail how in recent experimental implementations of driven CPBs the model in (1) together with various system-bath couplings according to (2) is realized and how the LS could be retrieved. In the set-ups studied in [20, 21, 36], a CPB with tunable charging energy E_C and Josephson energy E_J is subject to a microwave field and embedded in an environment which dominantly induces charge fluctuations. The Hamiltonian takes for large photon fields the form $H_{S,\text{CPB}}(t) = -\frac{1}{2}E_C\tau_z - \frac{1}{2}E_J\tau_x - \lambda\cos(\omega t)\tau_z$ with Pauli matrices $\{\tau_i\}$ and τ_z -coupling to the bath. (i) When the CPB is tuned close to its charge degeneracy $E_C = 0$, in the eigenstate representation of the CPB ($\tau_x \rightarrow \sigma_z$) one has a σ_z -term as in (1) with $E = E_J$. Within a rotating wave approximation near resonance $E_J \approx \hbar\omega$, also the driving term is obtained with $A = \lambda, \Omega = -\omega$. The operator $S(r)$ in (2) then reduces to transversal coupling $S(\pi/2) = \sigma_x$. (ii) Away from the charge degeneracy $E_C \neq 0$, longitudinal coupling $S(r \approx 0) = \sigma_z$ is achieved for strong driving $\lambda, \hbar\omega \gg E_J$ in the regime of multi-photon resonances $E_C = n\hbar\omega$ [20]. In the n -photon sector, $H_{S,\text{CPB}}(t)$ effectively reduces to (1) with $E = E_C$ and $A = -(E_J/2)J_n(2\lambda/\hbar\omega), \Omega = n\omega$ (for details see [34]).

Now, after the system has been prepared properly, its steady state in presence of the microwave drive according to a solution $\dot{\rho}_{\alpha\beta} = 0$ of (3) is probed with a weak pulse $H_P = \mu_P \cos(\omega_P t) \sigma_z, \mu_P \ll A$, to access the fundamental resonance at $\omega_{12} - \delta\omega_{12} = \omega_R - (\eta\omega_c/\pi)\Lambda^{(r)}$. The LS appears in the corresponding absorption spectrum upon varying either the detuning (see Fig. 1) or the amplitude (see Fig. 3) of the pump field (cf. [37]). For typical experimental parameters $E = 8$ GHz and $A = 0.8$ GHz, $\Omega = 7.5$ GHz [cf. Fig. 2], one finds a bare quasienergy gap $\omega_R \approx 1.7$ GHz and typical variations of vacuum fluctuations ($\eta = 0.1, \omega_c = 500$ GHz) in the range of $\delta\omega_{12}/\omega_R \approx 0.26$ for $r = 0$ and $\delta\omega_{12}/\omega_R \approx -0.23$ for $r = \pi/2$. These variations must be compared to the widths of the resonance lines which are determined by dressed dephasing/relaxation rates [36] and typically are much smaller, i.e., in the range of 10 MHz or less.

Cooper pair pump.— The devices discussed up to this point are tailored to externally manipulate their level structure. However, the LS may have also profound impact in superconducting circuits where transport properties are addressed. A specific example is a charge pump in form of the Cooper pair sluice [28, 38] sketched in Fig. 4a. It consists of a single superconducting island (CPB) separated by two SQUIDs with tunable Josephson energies $J_{L,R}(t)$. A third control parameter is provided by the gate charge $n_g(t)$ capacitively coupled to the is-

land. Full control of the quantum system is guaranteed via the three experimentally accessible parameters $J_{L,R}$ and n_g which allow for charge pumping when steered in a periodic protocol (see Fig. 4b). In the charging regime $E_C \gg \max\{J_L, J_R\}$ and close to a half integer of the gate charge $n_g(t)$, this device is described by a pseudospin-Hamiltonian [28, 39]

$$H_S(t) = -\frac{1}{2} \vec{\sigma} \cdot \vec{B}(t), \quad (6)$$

where $B_x(t) = J_+(t) \cos(\frac{\varphi}{2})$, $B_y(t) = J_-(t) \sin(\frac{\varphi}{2})$, $B_z(t) = E_C[2n_g(t) - 1]$ and $J_{\pm}(t) = J_L(t) \pm J_R(t)$. The total superconducting phase difference across the sluice is denoted by φ . The dominant source of noise are charge fluctuations implying a σ_z coupling to environmental modes.

This system has a more complex structure than the model (1); in particular it includes transversal and longitudinal driving. Its main observable is the charge Q_P pumped through the sluice during sequences of periodic driving cycles. Numerical results in steady state based on (3) are depicted in Fig. 4c with and without the LS versus the phase difference φ across the sluice. The latter one can be adjusted by an external magnetic field.

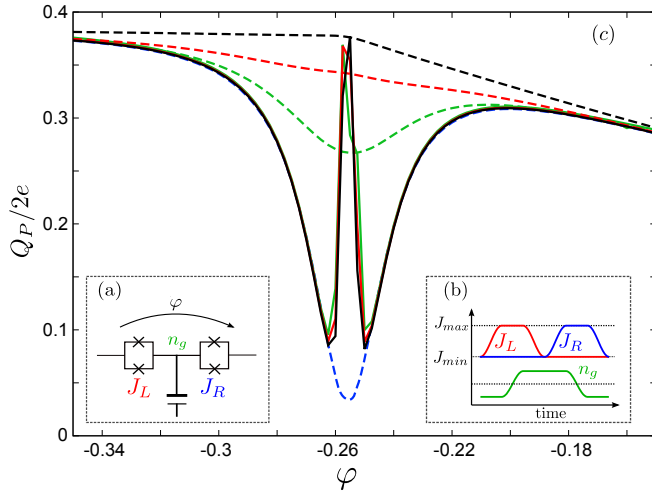


FIG. 4. (a) Schematic circuit diagram for the ‘sluice’ and (b) driving protocol with the three time-dependent control parameters $J_{L,R}$ and n_g for one pumping cycle. (c): Pumped charge Q_P with (solid) and without (dashed) LS contribution vs. phase φ for different values of the system-bath coupling: $\eta = 0.001$ (blue), $\eta = 0.005$ (green), $\eta = 0.01$ (red) and $\eta = 0.05$ (black). Parameters for the numerical simulations are: drive time $\tau = 1$ ns, $E_C = 1$ K, $\omega_c = 100$ GHz, $\Delta n_g = 0.2$, $J_{\max} = 0.1 E_C$, $J_{\min} = 10^{-3} J_{\max}$.

The pumped charge displays a very sensitive dependence on the phase difference which in turn determines the energy splitting. Close to a degeneracy of the quasienergies at $\varphi_c \approx -0.26$, one enters a regime where environmental effects on Q_P are strong and of order

$\eta\Omega/|\omega_{12} - \delta\omega_{12}|$ [23]. In contrast to the bare situation, however, the pumped charge including the LS depends only very weakly on the system-bath coupling. Namely, away from degeneracy (away from the peak), the LS enhances the level splitting so that renormalized dressed system properties prevail against decoherence. Noise induced transitions between the energy levels are thus suppressed and the pumped charge follows the bare one for $\eta = 0.001$. Within the domain of the bare crossing $\omega_{\alpha\beta} \approx 0$ (range of the peak), the steady state of (3) is completely determined by reservoir quantities, i.e., the LS and the Redfield tensor. Since both are proportional to η , the friction parameter drops out of the steady state equation. Apparently, within this latter range the predictions for Q_P with LS qualitatively deviate from those without LS giving rise to a peak instead of a dip. This analysis verifies the pronounced impact of vacuum fluctuations also on transport properties of superconducting circuits which may easily be accessible experimentally.

Conclusion.- We have presented a way to detect environmental zero-point fluctuations with broadband spectral densities in strongly driven quantum systems. Controlling the drive parameters, one can increase the relative strength of the system-reservoir coupling and, thus, enhance the induced LS to an extent unreachable in standard experiments. This LS displays distinctive signatures as a function of the driving amplitude and/or frequency. The predicted effect should be accessible in many solid-state systems, particularly in state of the art superconducting devices. Specific detection schemes have been discussed for a driven artificial atom realized as a CPB and for a circuit operated as a Cooper pair sluice. The proposed experimental protocols would shed new light on the impact of broadband environments on quantum systems at cryogenic temperatures which is completely absent in the classical regime.

Acknowledgements.- The authors would like to thank M. Günther and S. Pugnetti for fruitful discussions. This work has been supported by the German Science Foundation (DFG) within SFB/TRR-21 and AN336/6 as well as by the European Community’s Seventh Framework Programme (FP7/2007-2013) under grant agreement No. 228464 (MICROKELVIN). We gratefully acknowledge also financial support from the DAAD (V. G.) and the Finnish Graduate School in Nanoscience (S. G.). P. S. thanks for the support from FIRB - Futuro in Ricerca 2013 under Grant No. RBFR1379UX and FIRB 2012 under Grant No. RBFR1236VV HybridNanoDev.

* vera.gramich@uni-ulm.de

- [1] W. E. Lamb and R. C. Retherford, Phys. Rev. **72**, 241 (1947).
- [2] D. J. Heinzen and M. S. Feld, Phys. Rev. Lett. **59**, 2623 (1987).

- [3] M. Brune, P. Nussenzveig, F. Schmidt-Kaler, F. Bernardot, A. Maali, J. M. Raimond, and S. Haroche, *Phys. Rev. Lett.* **72**, 3339 (1994).
 - [4] M. Marrocco, M. Weidinger, R. T. Sang, and H. Walther, *Phys. Rev. Lett.* **81**, 5784 (1998).
 - [5] S. Haroche and J.-M. Raimond, *Exploring the Quantum: Atoms, Cavities, and Photons* (Oxford University Press, New York, 2006).
 - [6] A. Wallraff, D. I. Schuster, A. Blais, L. Frunzio, R.-S. Huang, J. Majer, S. Kumar, S. M. Girvin, and R. J. Schoelkopf, *Nature* **431**, 162 (2004).
 - [7] D. I. Schuster, A. A. Houck, J. A. Schreier, A. Wallraff, J. M. Gambetta, A. Blais, L. Frunzio, J. Majer, B. Johnson, M. H. Devoret, S. M. Girvin, and R. J. Schoelkopf, *Nature* **445**, 515 (2007).
 - [8] A. Blais, J. Gambetta, A. Wallraff, D. I. Schuster, S. M. Girvin, M. H. Devoret, and R. J. Schoelkopf, *Phys. Rev. A* **75**, 032329 (2007).
 - [9] D. I. Schuster, A. Wallraff, A. Blais, L. Frunzio, R.-S. Huang, J. Majer, S. M. Girvin, and R. J. Schoelkopf, *Phys. Rev. Lett.* **94**, 123602 (2005).
 - [10] J. M. Fink, M. Göppl, M. Baur, R. Bianchetti, P. J. Leek, A. Blais, and A. Wallraff, *Nature* **454**, 315 (2008).
 - [11] J. M. Fink, R. Bianchetti, M. Baur, M. Göppl, L. Steffen, S. Filipp, P. J. Leek, A. Blais, and A. Wallraff, *Phys. Rev. Lett.* **103**, 083601 (2009).
 - [12] A. Fragner, M. Göppl, J. M. Fink, M. Baur, R. Bianchetti, P. J. Leek, A. Blais, and A. Wallraff, *Science* **322**, 1357 (2008).
 - [13] C. M. Wilson, G. Johansson, A. Pourkabirian, M. Simoen, J. R. Johansson, T. Duty, F. Nori, and P. Delsing, *Nature* **479**, 376 (2011).
 - [14] P. Lähteenmäki, G. S. Paraoanu, J. Hassel, and P. J. Hakonen, *PNAS* **110**, 4234 (2013).
 - [15] C. J. Myatt, B. E. King, Q. A. Turchette, C. A. Sackett, D. Kielpinski, W. M. Itano, C. Monroe, and D. J. Wineland, *Nature* **403**, 269 (2000).
 - [16] D. Kielpinski, V. Meyer, M. A. Rowe, C. A. Sackett, W. M. Itano, C. Monroe, and D. J. Wineland, *Science* **291**, 1013 (2001).
 - [17] V. Gramich, P. Solinas, M. Möttönen, J. P. Pekola, and J. Ankerhold, *Phys. Rev. A* **84**, 052103 (2011).
 - [18] P. Solinas, M. Möttönen, J. Salmilehto, and J. P. Pekola, *Phys. Rev. B* **85**, 024527 (2012).
 - [19] K. W. Murch, U. Vool, D. Zhou, S. J. Weber, S. M. Girvin, and I. Siddiqi, *Phys. Rev. Lett.* **109**, 183602 (2012).
 - [20] W. D. Oliver, Y. Yu, J. C. Lee, K. K. Berggren, L. S. Levitov, and T. P. Orlando, *Science* **310**, 1653 (2005).
 - [21] C. M. Wilson, T. Duty, F. Persson, M. Sandberg, G. Johansson, and P. Delsing, *Phys. Rev. Lett.* **98**, 257003 (2007).
 - [22] A. Izmalkov, S. H. W. van der Ploeg, S. N. Shevchenko, M. Grajcar, E. Il'ichev, U. Hübner, A. N. Omelyanchouk, and H.-G. Meyer, *Phys. Rev. Lett.* **101**, 017003 (2008).
 - [23] S. Gasparinetti, P. Solinas, S. Pugnetti, R. Fazio, and J. P. Pekola, *Phys. Rev. Lett.* **110**, 150403 (2013).
 - [24] T. M. Stace, A. C. Doherty, and S. D. Barrett, *Phys. Rev. Lett.* **95**, 106801 (2005).
 - [25] T. M. Stace, A. C. Doherty, and D. J. Reilly, *Phys. Rev. Lett.* **111**, 180602 (2013).
 - [26] A. J. Ramsay, T. M. Godden, S. J. Boyle, E. M. Gauger, A. Nazir, B. W. Lovett, A. M. Fox, and M. S. Skolnick, *Phys. Rev. Lett.* **105**, 177402 (2010).
 - [27] J. I. Colless, X. G. Croot, T. M. Stace, A. C. Doherty, S. D. Barrett, H. Lu, A. C. Gossard, and D. J. Reilly, *arXiv:1305.5982v1 [cond-mat.mes-hall]* (2013).
 - [28] A. O. Niskanen, J. P. Pekola, and H. Seppä, *Phys. Rev. Lett.* **91**, 177003 (2003).
 - [29] M. Möttönen, J. J. Vartiainen, and J. P. Pekola, *Phys. Rev. Lett.* **100**, 177201 (2008).
 - [30] S. Gasparinetti, P. Solinas, and J. P. Pekola, *Phys. Rev. Lett.* **107**, 207002 (2011).
 - [31] S. Gasparinetti, P. Solinas, Y. Yoon, and J. P. Pekola, *Phys. Rev. B* **86**, 060502(R) (2012).
 - [32] M. O. Scully and M. S. Zubairy, *Quantum Optics* (Cambridge University Press, 1997).
 - [33] M. Grifoni and P. Hänggi, *Physics Reports* **304**, 229 (1998).
 - [34] See Supplemental at XXX for details on the LS and the Floquet master equation.
 - [35] A. Russomanno, S. Pugnetti, V. Brosco, and R. Fazio, *Phys. Rev. B* **83**, 214508 (2011).
 - [36] C. M. Wilson, G. Johansson, T. Duty, F. Persson, M. Sandberg, and P. Delsing, *Phys. Rev. B* **81**, 024520 (2010).
 - [37] M. Silveri, J. Tuorila, M. Kemppainen, and E. Thuneberg, *Phys. Rev. B* **87**, 134505 (2013).
 - [38] A. O. Niskanen, J. M. Kivioja, H. Seppä, and J. P. Pekola, *Phys. Rev. B* **71**, 012513 (2005).
 - [39] P. Solinas, M. Möttönen, J. Salmilehto, and J. P. Pekola, *Phys. Rev. B* **82**, 134517 (2010).
-

Supplemental Material

In this supplemental material to our article ‘Lamb shift enhancement and detection in strongly driven superconducting circuits’ we present further details about the derivation of the Lamb shift as well as the semiclassical Rabi model and its equivalence to experimental realizations.

Derivation of the Lamb shift

To reveal the impact of the Lamb shift expression given in Eq. (4) in the main text, we present here its full derivation, starting with the time-independent Floquet master equation (for further details follow the steps in, e.g., Refs. [1–3]) written in the basis of Floquet modes $|\Phi_\alpha(t)\rangle = |\Phi_\alpha(t + \frac{2\pi}{\Omega})\rangle$ and in the Schrödinger picture

$$\dot{\rho}_{\alpha\beta}(t) = -i(\omega_{\alpha\beta} - \delta\omega_{\alpha\beta})\rho_{\alpha\beta}(t) + \sum_{\gamma,\delta} \mathcal{R}_{\alpha\beta\gamma\delta} \rho_{\gamma\delta}(t), \quad (7)$$

where

$$\mathcal{R}_{\alpha\beta\gamma\delta} = \Gamma_{\alpha\gamma\beta\delta}^+ + \Gamma_{\alpha\gamma\beta\delta}^- - \delta_{\delta,\beta} \sum_{\mu} \Gamma_{\mu\gamma\mu\alpha}^+ - \delta_{\gamma,\alpha} \sum_{\mu} \Gamma_{\mu\beta\mu\delta}^- \quad (8)$$

represents the “Redfield” tensor and

$$\Gamma_{\alpha\beta\gamma\delta}^+ = \frac{1}{\hbar} \sum_k \mathcal{S}(\Delta_{\alpha\beta,k}) X_{\alpha\beta,k} (X_{\gamma\delta,k})^*, \quad \Gamma_{\alpha\beta\gamma\delta}^- = \frac{1}{\hbar} \sum_k \mathcal{S}(\Delta_{\gamma\delta,k}) X_{\alpha\beta,k} (X_{\gamma\delta,k})^* \quad (9)$$

the effective relaxation and dephasing rates for a $T = 0$ - environment, respectively. A crucial point in deriving the result (7) is that we have performed the so-called partial secular approximation [3]. It consists in retaining all terms which oscillate with $\epsilon_\alpha \neq \epsilon_\beta$ (in contrast to the usual rotating wave approximation) and neglecting only those with multiple integers k_α, k_β of $\hbar\Omega$ where $k_\alpha \neq k_\beta$. The Lamb shift contributions $\delta\omega_{\alpha\beta}$ arise from principal value terms via $\int_0^\infty dt e^{i\omega t} = \pi\delta(\omega) + i\mathcal{P}(1/\omega)$ in the Floquet master equation in the basis of Floquet states $|\Psi_\alpha(t)\rangle$ following the procedure outlined in Refs. [2, 3]. The matrix elements $X_{\alpha\beta,k} = \frac{\Omega}{2\pi} \int_0^{2\pi/\Omega} dt e^{-ik\Omega t} \langle \Phi_\alpha(t) | S | \Phi_\beta(t) \rangle$ with the driving frequency Ω contain the system operator S coupling to the reservoir and obey the symmetry relation $X_{\alpha\beta,k} = X_{\beta\alpha,-k}^*$. The latter one helps to simplify the Lamb shift terms. Transition energies are given by

$$\hbar\Delta_{\alpha\beta,k} = \epsilon_\alpha - \epsilon_\beta + k\hbar\Omega \quad (10)$$

with $\epsilon_i(t), i = \alpha, \beta$ playing the role of a dressed state energy. The quantity $\omega_{\alpha\beta} = (\epsilon_\alpha - \epsilon_\beta)/\hbar$ thereby expresses the Floquet quasienergy gap which is a non-dissipative contribution of the driven quantum system. In the above formulas we have also used the abbreviation

$$\mathcal{S}(\omega) = \theta(\omega)J(\omega)n_{\text{th}}(\omega) + \theta(-\omega)J(-\omega)[n_{\text{th}}(-\omega) + 1] \quad (11)$$

containing the spectral bath density $J(\omega)$ in units of an energy. Here, $\theta(\omega)$ denotes the Heavyside function and $n_{\text{th}}(\omega)$ is the usual Bose-Einstein distribution.

In the above derivation we have neglected principal value corrections to the rates in Eq. (9) which are much smaller compared to the Lamb shift contributions we are interested in. In the singular coupling limit the Lamb shift is the leading order correction of the system dynamics which is completely determined by the bath at the degeneracy point ($\omega_{\alpha\beta} \approx 0$), while the dominant parts of the rates are already captured by (9). In other words, for the Lamb shift we only take into account terms which renormalize transition frequencies in the form $\omega_{\alpha\beta} - \delta\omega_{\alpha\beta}$. To evaluate them explicitly, one has to consider integrals of the form

$$I_{\text{PV}}^\pm(\Delta_{\alpha\beta,k}) = \mathcal{P} \int_0^\infty d\omega \frac{J(\omega)n_{\text{th}}(\pm\omega)}{\omega - \Delta_{\alpha\beta,k}}. \quad (12)$$

This leads us to the following expression:

$$\begin{aligned} \delta\omega_{\alpha\beta} = & \frac{1}{\pi\hbar} \sum_{\mu,k} [|X_{\beta\mu,k}|^2 \{I_{\text{PV}}^+(\Delta_{\mu\beta,-k}) + I_{\text{PV}}^-(\Delta_{\beta\mu,k})\} \\ & - |X_{\mu\alpha,k}|^2 \{I_{\text{PV}}^+(\Delta_{\mu\alpha,k}) + I_{\text{PV}}^-(\Delta_{\alpha\mu,-k})\}] . \end{aligned} \quad (13)$$

The above results apply to arbitrary spectral density of the bath $J(\omega)$. In the sequel, we assume an Ohmic-type distribution with exponential cut-off $J(\omega) = \eta \hbar \omega \exp(-\omega/\omega_c)$ with a dimensionless coupling constant η and a large cut-off frequency ω_c . At $T \rightarrow 0$, where $\delta\omega_{\alpha\beta}$ only accounts for environmental vacuum fluctuations [4], $I_{\text{PV}}^+(\Delta_{\alpha\beta,k}) \rightarrow 0$ and

$$I_{\text{PV},T=0}^-(\Delta_{\alpha\beta,k}) = -\eta \hbar \omega_c + \eta \hbar \Delta_{\alpha\beta,k} e^{-\Delta_{\alpha\beta,k}/\omega_c} \text{Ei}(\Delta_{\alpha\beta,k}/\omega_c) \quad (14)$$

with $\text{Ei}(z) = -\int_{-z}^{\infty} dy e^{-y}/y$, where the integral is understood in the principal value sense. The terms linear in ω_c in (14) describing the static effect of the bath do not contribute to the Lamb shift [5] as they cancel each other. Finally, the Lamb shift in the zero temperature case yields in general

$$\delta\omega_{\alpha\beta}^{T=0} = \frac{\eta}{\pi} \sum_{\mu,k} [\Delta_{\beta\mu,k} f(\Delta_{\beta\mu,k}/\omega_c) |X_{\beta\mu,k}|^2 - \Delta_{\alpha\mu,-k} f(\Delta_{\alpha\mu,-k}/\omega_c) |X_{\mu\alpha,k}|^2], \quad (15)$$

where we have introduced the function $f(x) = \text{Ei}(x)\exp(-x)$ with the property $f(x) \rightarrow C_\gamma + \ln(x)$ for $x \ll 1$ with the Euler constant C_γ . Therewith, in the limit $\Omega/\omega_c \ll 1$ (i.e., for large cut-off ω_c), one recovers logarithmic behaviour known from the quantum optical Lamb shift [6].

Now we restrict ourselves to a TLS ($\mu = 1, 2$). Then, taking into account the symmetry relations $X_{\alpha\beta,k} = X_{\beta\alpha,-k}^*$ as well as $X_{11,k} = -X_{22,k}$ for a traceless noise operator (which is true for all combinations of Pauli matrices) and orthogonal Floquet modes at all times, we arrive with the definition $g(x) = x[f(x) + f(-x)]$ at Eq. (4) given in the main text.

Semiclassical Rabi model

We consider here details of the semiclassical Rabi model serving which, despite its simplicity, describes recent experimental realizations, see below and (see, e.g., [7–9]). The Hamiltonian is given by

$$H(t) = \begin{pmatrix} -\frac{E}{2} & A^* e^{i\Omega t} \\ A e^{-i\Omega t} & \frac{E}{2} \end{pmatrix} = -\frac{E}{2} \sigma_z + A \{\cos(\Omega t) \sigma_x - \sin(\Omega t) \sigma_y\}, \quad (16)$$

where for simplicity the driving amplitude A is taken as real-valued and E is the bare energy level spacing. To find the solution of the Schrödinger equation, we follow a standard procedure: First, moving to a rotating frame reveals a time-independent Hamiltonian which we diagonalize. In a second step, we revert to the laboratory frame and cast the solutions finally in Floquet form. The so-found quasienergies are $\epsilon_{1,2} = (\Delta \pm \hbar\omega_R)/2$ with detuning $\Delta = E - \hbar\Omega$ and $\omega_R = \frac{1}{\hbar} \sqrt{\Delta^2 + 4|A|^2}$ being the Rabi frequency.

The corresponding Floquet modes are:

$$|\phi_1(t)\rangle = \begin{pmatrix} \cos \theta \\ -e^{-i\Omega t} e^{i\phi} \sin \theta \end{pmatrix} \quad (17)$$

$$|\phi_2(t)\rangle = \begin{pmatrix} e^{-i\phi} \sin \theta \\ e^{-i\Omega t} \cos \theta \end{pmatrix} \quad (18)$$

where $\phi = -\arg A$ and $\tan(2\theta) = \frac{2|A|}{\Delta}$.

As we have chosen A to be real, one has $\phi = 0$. The coupling matrix elements $X_{\alpha\beta,k}^{(r)}$ are obtained in the following way: For σ_z -noise only terms with $k = 0$ survive with

$$X_{11,0}^{(0)} = \cos^2 \theta - \sin^2 \theta = \cos 2\theta = -X_{22,0}^{(0)} \quad (19)$$

$$X_{21,0}^{(0)} = 2 \sin \theta \cos \theta = \sin 2\theta = X_{12,0}^{*(0)}. \quad (20)$$

Together with Eq. (4) in the main text, this then leads to $\Lambda^{(0)}$. For σ_x -noise, the non-zero contributions $k = \pm 1$ provide the coefficients

$$X_{11,-1}^{(\pi/2)} = -\frac{1}{2} \sin 2\theta = X_{11,1}^{(\pi/2)}, \quad X_{22,-1}^{(\pi/2)} = X_{22,1}^{(\pi/2)} = -X_{11,1}^{(\pi/2)} \quad (21)$$

$$X_{12,-1}^{(\pi/2)} = \cos^2 \theta = X_{21,1}^{*(\pi/2)}, \quad X_{21,-1}^{(\pi/2)} = -\sin^2 \theta = X_{12,1}^{*(\pi/2)}, \quad (22)$$

which yields $\Lambda^{(\pi/2)}$ [Eq. (5) in the main text].

Mapping to the Rabi model

As discussed in the main text, recent experiments with driven CPBs are described with

$$H_{S,\text{CPB}}(t) = -\frac{1}{2}E_C\tau_z - \frac{1}{2}E_J\tau_x - \lambda\cos(\omega t)\tau_z \quad (23)$$

with tunable charging energy E_C and Josephson energy E_J [7–9]. The coupling to the reservoir is dominated by charge noise and thus proportional to τ_z . Here, we show how from $H_{S,\text{CPB}}(t)$ the Rabi model (16) with various coupling mechanisms to the environment is obtained.

Transversal coupling: Close to charge degeneracy $E_C = 0$, one gains the Rabi model in the eigenstate representation of the CBP, i.e., $\tau_x \rightarrow \sigma_z$ and $\tau_z \rightarrow -\sigma_x$, within a rotating wave approximation. The drive parameters then read $A = \lambda$ and $\Omega = -\omega$. The coupling to the bath is transversal with $S(r = \pi/2) = \sigma_x$. The pointer operator is determined by $\tan(r) = E_J/E_C$. Tuning the CPB to its charge degeneracy $E_C = 0$, thus implies $S(\pi/2) = \sigma_x$, while away from this point the system-bath coupling tends towards $S(0) = \sigma_z$.

Longitudinal coupling: For $E_C \neq 0$ (away from charge degeneracy) and for strong driving $\lambda, \hbar\omega \gg E_J$, a dressed tunneling picture applies. Accordingly, a unitary transformation $U(t) = \exp[-i\phi(t)\tau_z/(2\hbar)]$ with $\dot{\phi}(t) = 2\lambda\cos(\omega t)$ leads to $\dot{H}_{S,\text{CPB}}(t) = U^\dagger H_{S,\text{CPB}}(t)U(t) + i\hbar U^\dagger(t)\dot{U}(t)$, where the driving appears in the tunneling term, i.e., $E_J\tau_x - \lambda\cos(\omega t)\tau_z \rightarrow E_J[e^{i\phi(t)/\hbar}\tau_+ + e^{-i\phi(t)/\hbar}\tau_-]$. By decomposing the time-dependent phase factors in terms of Bessel functions using the Jacobi-Anger expansion $\exp(iz\sin\varphi) = \sum_{n=-\infty}^{\infty} J_n(z)\exp(in\varphi)$, one may put near the n -photon resonance $E_C = n\hbar\omega$ within a rotating wave approximation $e^{i\phi(t)/\hbar} \approx J_n(2\lambda/\hbar\omega)e^{in\omega t}$. This way, one obtains the Rabi model with $E = E_C$ and drive parameters $A = -(E_J/2)J_n(2\lambda/\hbar\omega)$, $\Omega = n\omega$. As the transformation $U(t)$ commutes with the CBP-bath coupling operator, in the rotating frame the environment leads to pure dephasing only (longitudinal coupling).

* vera.gramich@uni-ulm.de

- [1] R. Blümel, A. Buchleitner, R. Graham, L. Sirko, U. Smilansky, and H. Walther, Phys. Rev. A **44**, 4521 (1991).
- [2] M. Grifoni and P. Hänggi, Physics Reports **304**, 229 (1998).
- [3] S. Gasparinetti, P. Solinas, S. Pugnetti, R. Fazio, and J. P. Pekola, Phys. Rev. Lett. **110**, 150403 (2013).
- [4] It is also justified to work with the zero-temperature expression for the Lamb shift at finite, but low T due to the exponential suppression of the temperature dependence, which can be seen by analyzing Eq. (12).
- [5] A. Santana, J. M. Gomez Llorente, and V. Delgado, J. Phys. B: At. Mol. Opt. Phys. **34**, 2371 (2001).
- [6] W. E. Lamb and R. C. Retherford, Phys. Rev. **72**, 241 (1947).
- [7] W. D. Oliver, Y. Yu, J. C. Lee, K. K. Berggren, L. S. Levitov, and T. P. Orlando, Science **310**, 1653 (2005).
- [8] C. M. Wilson, T. Duty, F. Persson, M. Sandberg, G. Johansson, and P. Delsing, Phys. Rev. Lett. **98**, 257003 (2007).
- [9] C. M. Wilson, G. Johansson, T. Duty, F. Persson, M. Sandberg, and P. Delsing, Phys. Rev. B **81**, 024520 (2010).